JOURNAL OF APPLIED ELECTROCHEMISTRY 19 (1989) 677–682

Modelling of gas-evolving electrolysis cells. II. Investigation of the flow field around gas-evolving electrodes*

M. KUHN‡, G. KREYSA§

Dechema-Institute, Theodor-Heuss-Allee 25, D-6000 Frankfurt am Main 97, FRG

Received 25 July 1988; revised 2 February 1989

The flow field in front of and around hydrogen- or oxygen-evolving electrodes of different shapes has been investigated by Laser–Doppler anemometry. A strong influence of geometrical parameters on the structure of the flow field has been found. The vertical velocity component in front of a plane electrode decreases with distance. Due to the resulting pressure gradient a well-defined bubble curtain is formed at such electrodes. Gas voidage data derived from experimental velocity data are in close agreement with the predictions of the coalescence barrier model which is valid for electrolyte solutions.

Nomenclature

f	frequency (s^{-1})
F	Faraday number (96 487 As mol^{-1})
G	volumetric gas flow rate ($cm^3 s^{-1}$)
h	height (cm)
i	current density ($A cm^{-2}$)
L	volumetric liquid flow rate ($cm^3 s^{-1}$)
N	number of data points (1)
p	pressure (Pa)
Q_t	total volumetric flow rate ($cm^3 s^{-1}$)
R_g	gas constant (8.3144 $J K^{-1} mol^{-1}$)
T	temperature (K)
Tu	degree of turbulence (1)
u	linear flow velocity ($cm s^{-1}$)
u^0	superficial flow velocity ($cm s^{-1}$)
u_{sw}	swarm velocity ($cm s^{-1}$)
x	thickness (cm)
y	depth (cm)

Greek symbols

ε_g	gas voidage (1)
ε_m	maximum gas voidage (1)
ν_e	electron number (1)
ϱ	mass density ($g cm^{-3}$)

1. Introduction

In Part I [1] a new model describing the gas voidage in gas-evolving electrolysis cells was presented. Based on the empirical experience that bubble coalescence is hindered in such situations, the derived equations allow the calculation of the gas voidage as a function of the superficial gas velocity based on a semi-empirical coalescence barrier model. Experimental investigations confirm the theoretical prediction of the existence of a limiting gas voidage which is a characteristic quantity of each gas/electrolyte combination. Electrolysis experiments under microgravity show a remarkable smaller mean bubble diameter [2]. Under these circumstances coalescence is strongly hindered. The lack of the buoyancy force and, therefore, kinetic energy leads, as a consequence of the coalescence barrier, to a complete prevention of coalescence. Investigations of the macroscopic properties of electrogenerated bubble flow show that full understanding of the effects requires knowledge about microscopic properties, the structure and the velocity of the bubble flow at the electrode. The flow field interacts with major parameters of a gas-evolving reaction such as gas voidage, bubble size, thickness of the diffusion layer and mass and heat transfer [3–8].

There are a few models in the literature describing the flow field structure [8–10] and the authors used the assumptions of their models for determination of gas voidage and interelectrode resistance, respectively. The present paper presents measurements of the flow field at and around a gas-evolving electrode. Hydrogen and oxygen evolution in alkaline solution at different electrode shapes were investigated.

The experimental results were obtained by means of Laser–Doppler anemometry (LDA) [11, 12]. This technique is superior because there is no interaction with the system under test in contrast to impact probes (e.g. hot wire anemometry) and the dimensions of the measuring control volume are very small compared

* Paper presented at the 2nd International Symposium on Electrolytic Bubbles organized jointly by the Electrochemical Technology Group of the Society of Chemical Industry and the Electrochemistry Group of the Royal Society of Chemistry and held at Imperial College, London, 31st May and 1st June 1988.

‡ Present address: Digital Equipment GmbH, Hahnstraße 25, D-6000 Frankfurt am Main, FRG.

§ Author to whom correspondence should be addressed.

0021-891X/89 $03.00 + .12

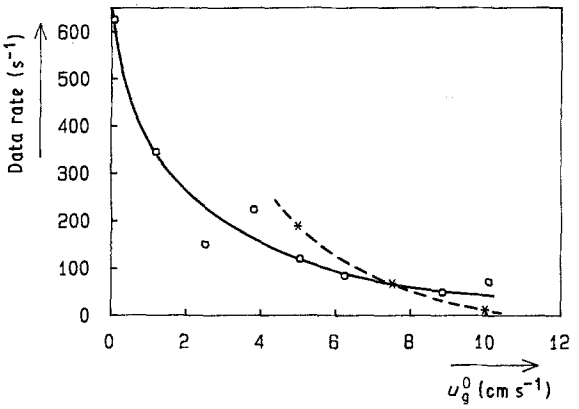

Fig. 1. Obtainable data rates by LDA measurements as function of superficial gas velocity [13]: (○) air/water, (*) air/water with 1% methanol.

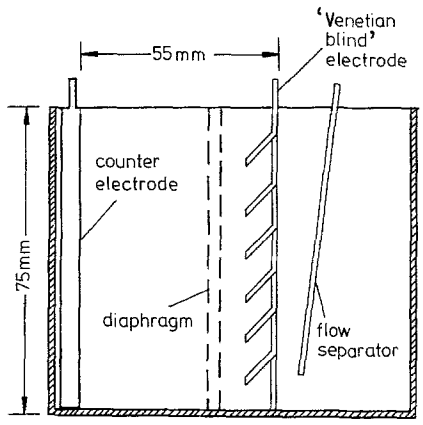

Fig. 2. Schematic view of the electrolysis cell used for LDA measurements.

with other non-impact methods (ultrasonic Doppler anemometry) and yields the geometrical resolution of the velocity measurement, which is necessary for investigations in flow fields at gas-evolving electrodes.

The major shortcoming of the method is the strong dependence of the rate of measureable events on the transparency of the two-phase flow. An interruption of one or both of the inclined laser beams outside the measuring control volume by bubbles in the bulk of the solution, or adhering at the walls of the cell, leads to dropouts of the measuring system.

There have been investigations in bubble columns which show this dependence between superficial gas velocity and the resulting data aquisition rate [13].

Figure 1 shows the strong drop in data rate with ascending superficial gas velocity [13]. This means the data aquisition rate decreased with increasing gas voidage. In coalescence-preventing solutions a measurement through 90 mm of bubble flow with more than 110 mm s^{-1} superficial gas velocity is almost impossible due to the very low data rate. However, by appropriate design of the system under test investigations in two-phase flow with gas voidage up to $\varepsilon_g = 0.25$ are possible [14–16].

Due to the small diameter of electrogenerated bubbles, which are of the same order of magnitude as the tracer substances used in single phase flow LDA measurements [9, 13], and the small difference between liquid and bubble velocity, a treatment of the gas/liquid flow as a single phase flow is possible [16–18].

The occurrence of more than one particle in the measuring control volume gives interference of the scattered light. If there are two particles their scattered frequencies, f_1 and f_2, wil superimpose. The frequency resulting from interference is described by Equation 1

$$f = (f_1 + f_2)/2 \qquad (1)$$

with $f_1 \approx f_2$ [19].

If it is guaranteed that the shift frequency used in the LDA measurement is great compared to the deviations resulting from the Doppler effect, the interference of scattered light results in a mean frequency response and, by evaluation of the raw data, in a mean velocity of the contributing particles.

2. Experimental details

As model systems of gas-evolving electrodes hydrogen and oxygen evolution on nickel electrodes were chosen. The cell stood inside a Perspex trough with the inside dimensions, width 120 mm, height 105 mm and depth 60 mm. The cell, which is shown in Fig. 2, was 5 mm in depth, parallel to the laser beams.

The active surface of the electrode was, in the case of flat plates, 5.75 cm^2. The applied current of 5 A corresponded to a current density of 8.7 kA m^{-2}. All experiments were conducted with 0.71 of 30% KOH solution at a temperature of 65° C, which was the equilibrium temperature for the system under current. Before the measurements 2 h of pre-electrolysis were carried out. The LDA system consisted of a 15 mW He–Ne laser (NEC gas laser), an optoacoustic Modulation and Transmitting System (OEI LD-OK-H111) and a receiving system, consisting of a light-collecting lens, a diaphragm and a photomultiplier. Data treatment was performed by a bandpass filter (OEI Variable Bandpass-Filter), a transient recorder (Iwatsu DM 901), a zero-detector (OEI DataProcessor-System) and a microcomputer (Heath-Zenith H-88). The system controlled the measurement and evaluated the data. It was driven with a frequency shift of 0.5 MHz. For this system a velocity of 20 cm s^{-1} resulted in a frequency difference of 52 kHz. This means the resulting Doppler frequency variations were small compared with the shift frequency and Equation 1 is valid. The bandpass filter was operated with the limits 100 kHz and 4 MHz. Two particle detections were separated by a break of at least 20 ms, in order to avoid double detection of one particle. 500–1000 measuring events were collected to determine the mean velocity at one position.

3. Results and discussion

The vertical velocity component of the flow field at a flat plate electrode was studied for hydrogen and oxygen evolution with different distances between electrode and separator. Additionally, for a 'Venetian blind' electrode vertical and horizontal velocity components were determined.

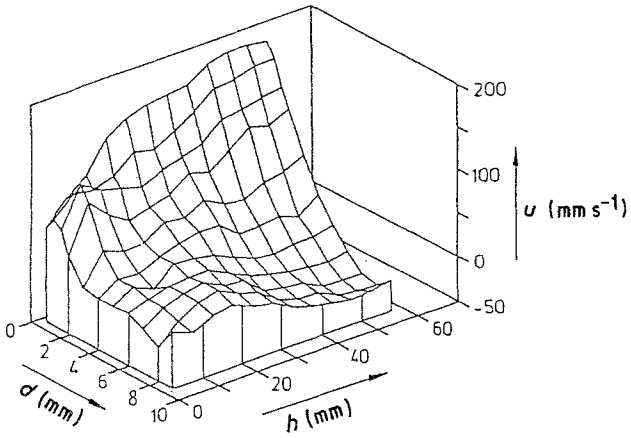

Fig. 3. Vertical velocity distribution at a hydrogen-evolving flat plate electrode in 30% KOH; distance electrode–separator: 10 mm; $i = 8.7\,\mathrm{kA\,m^{-2}}$; $T = 65°\mathrm{C}$.

3.1. *Flow field at flat plate electrodes*

At the flat plate electrodes the horizontal velocity of the bubble flow was very small and strongly fluctuating, therefore a measurement within reasonable time was impossible.

Figures 3 and 4 show the vertical flow velocity distributions for hydrogen and oxygen evolution, respectively. The profiles of the velocity distributions are very similar in shape. They show a velocity increase with height, which is less pronounced than linear. The region of upwards and downwards directed flow can be clearly distinguished. At the front of the electrode velocities of nearly $20\,\mathrm{cm\,s^{-1}}$ are observed. The difference between the two distributions is much smaller than one would expect on the basis of the superficial gas velocities, which are 2 : 1 for identical electrochemical conditions. Therefore the velocity of the bubble flow is influenced by hydrodynamic effects to a much greater extent than by the volumetric rate of gas production.

At smaller distances between electrode and separator, the two opposite directed flows in this channel interact to an increasing extent. This leads to higher turbulence in the flow field and reduced velocities. Nevertheless, the similarity between the velocity distribution profiles for hydrogen and oxygen evolution

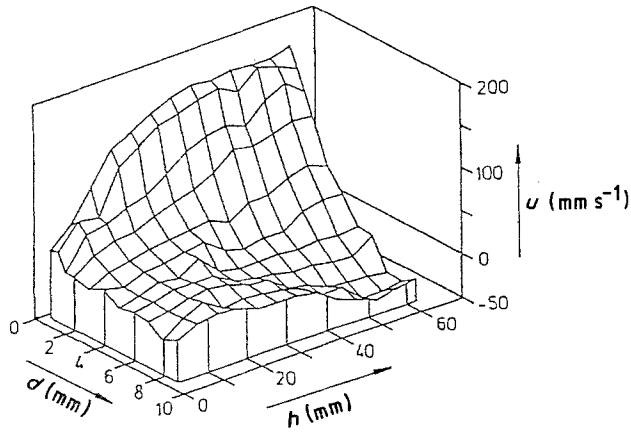

Fig. 4. Vertical velocity distribution at an oxygen-evolving flat plate electrode in 30% KOH; distance electrode–separator: 10 mm; $i = 8.7\,\mathrm{kA\,m^{-2}}$; $T = 65°\mathrm{C}$.

was preserved while varying the width of the flow channel between electrode and separator.

All velocity distributions show a sharp drop in the vertical component with increasing distance from the electrode surface. The effect of such a velocity gradient in a flow field is described by Bernoulli's law. For a flow in steady state at each point in the flow field the sum of the static and dynamic pressure is equal [20]. Considering two locations in the flow field at a given height, h, it follows that

$$p_1 + \frac{\varrho}{2} u_1^2 = p_2 + \frac{\varrho}{2} u_2^2 \qquad (2)$$

With $u_1 > u_2$, one can deduce from Equation 2 that $p_1 < p_2$. This pressure difference between parts of the flow field with different flow velocities results in a force directed towards the locations of higher flow velocities. Considering the flow fields shown in Figs 3 and 4 there will be a pressure gradient perpendicular to the electrode surface resulting in a force directed towards the electrode. The build-up of a well-defined thin layer of bubble flow – like a bubble curtain – at the electrode surface, which is found in almost all similar systems, is due to this force.

3.2. *Determination of superficial velocity and gas voidage data*

The velocity data of the flow field in front of a flat plate electrode were used for determination of the characteristic quantities of the bubble flow (e.g. volumetric flow rate, superficial velocity and gas voidage). For calculation of the total volumetric flow rate, Q_t, of the upwards directed flow the measured vertical velocity components, u_v, between the limits of the electrode surface ($x = 0$) and the point of flow direction reversal ($x = x'$) were numerically integrated (Equation 3)

$$\int_0^{x'} y u_v(x)\,\mathrm{d}x = Q_t(h) \qquad (3)$$

with $y = 5\,\mathrm{mm}$, the depth of the electrochemical cell. Assuming a uniform current distribution at the electrode, and that the total volumetric flow rate is given by Equation 3, the volumetric liquid flow rate, $L(h)$, can also be calculated by means of the following equation

$$Q_t(h) = L(h) + G(h) = L(h) + \int_0^h i \frac{R_g T}{p v_e F} y\,\mathrm{d}h \qquad (4)$$

With the thickness, x', of the upward flow the superficial velocities of both phases can also be determined

$$u_g^0 = \frac{G(h)}{x'y}; \quad u_l^0 = \frac{L(h)}{x'y} \qquad (5)$$

Figures 5 and 6 show calculated gas and liquid superficial velocities.

For both hydrogen and oxygen evolution the variations of the superficial velocities with height resemble each another. The increase in the liquid superficial velocities becomes smaller with height until the slope approaches linearity. The mean gas voidage of the

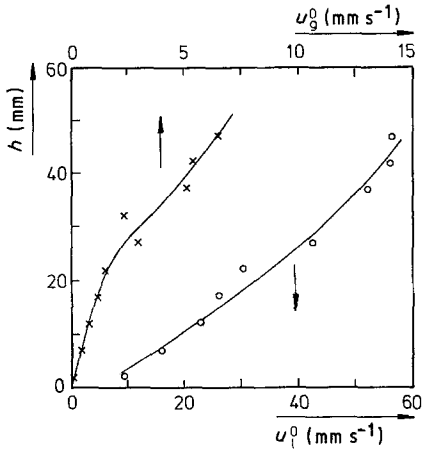

Fig. 5. Gas and liquid superficial velocities as function of electrode height for oxygen evolution at flat plate nickel electrode; 30% KOH; distance electrode–separator: 10 mm (calculated from velocity data in Fig. 4).

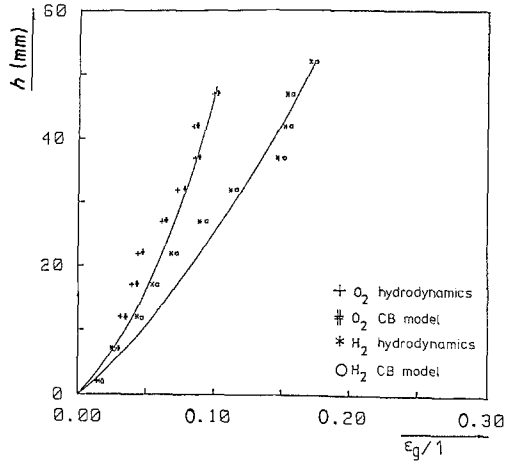

Fig. 7. Mean gas voidage as a function of electrode height for oxygen and hydrogen evolution at a flat nickel electrode; 30% KOH; distance electrode-separator: 10 mm.

bubble flow can be obtained in two ways. Iterative solution of Equation 6, which is presented and explained in Part I [1], yields the gas voidage if the maximum gas voidage and the rise velocity of a single bubble are known.

$$\varepsilon_g = \frac{\varepsilon_m}{\left(1 + \frac{u_l^0\left(\frac{\varepsilon_m - \varepsilon_g}{1 - \varepsilon_g}\right) + \varepsilon_m u_{sw}}{u_g^0}\right)} \qquad (6)$$

The bubble swarm velocity, u_{sw}, is calculated introducing the rise velocity of a single bubble and the reduced gas voidage ($\varepsilon_g/\varepsilon_m$) into the Marucci equation [1]. Typical swarm velocities are of the order of 10 mm s^{-1}, which is small compared to the measured flow rates of the two phase mixtures given in Figs 3 and 4. For calculation of ε_g the u_l^0 and u_g^0 data were taken from Figs 5 and 6; ε_m and the single bubble rise velocities were taken from independent measurements [1].

Based on the assumption of a negligible swarm velocity a second method of gas voidage calculation is possible

$$\varepsilon_g = \frac{G(h)}{Q_l(h)} \qquad (7)$$

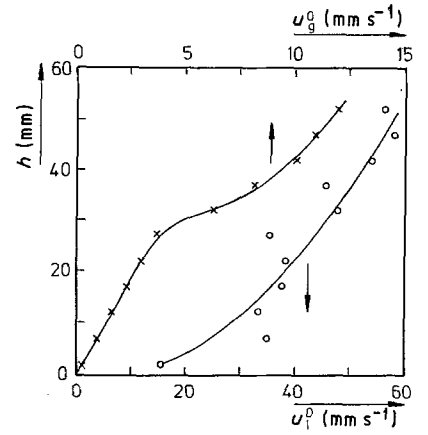

Fig. 6. Gas and liquid superficial velocities as function of electrode height for hydrogen evolution at flat plate nickel electrode; 30% KOH; distance electrode–separator: 10 mm (calculated from velocity data in Fig. 3).

where $G(h)$ is given by the integral in Equation 4 and $Q_l(h)$ by Equation 3.

In Fig. 7 gas voidage data calculated by these two methods (by Equations 3–5 and 7 indicated as hydrodynamics, by Equation 6 indicated as CB model) are represented. There is always only a small deviation between these two methods of determination. All the voidage data obtained are lower than the maximum gas voidages which are $\varepsilon_m = 0.13$ for oxygen and $\varepsilon_m = 0.24$ for hydrogen [1]. The solid lines are estimated curves fixed at the origin just to group the data into hydrogen and oxygen evolution. The close agreement between the two methods of gas voidage determination demonstrates the reliability of the coalescence barrier mode (Equation 6).

3.3. *Flow field at a 'Venetian blind' electrode*

To get an impression of the flow field structure at electrodes used in industrial electrolyzers, the bubble flow at a 'Venetian blind' nickel electrode was investigated. The use of a separator wall behind the electrode avoids the interference of the diametrically oriented flows (upwards and downwards). The distance between the electrode and the separator wall increased with cell height and should assist the transport of the evolved gas behind the electrode. At this electrode both velocity components, vertical and horizontal, were measured. Figure 8 shows the distribution of the vertical velocity components.

Already at a height of 40 mm vertical velocities of more than 20 cm s^{-1} are observed in the flow channel behind the electrode. Based on gas-lift action this stream forces the gas/solution mixture from the front to the backside space of the electrode and quickly removes the bubbles from the electrolysis zone.

A measurement of both velocity components at identical positions was impossible due to geometrical restrictions by the electrode and the two laser beams. For presentation of the magnitude and direction of the velocity vectors an interpolation of the measured vectorial components onto an artificial grid was necessary.

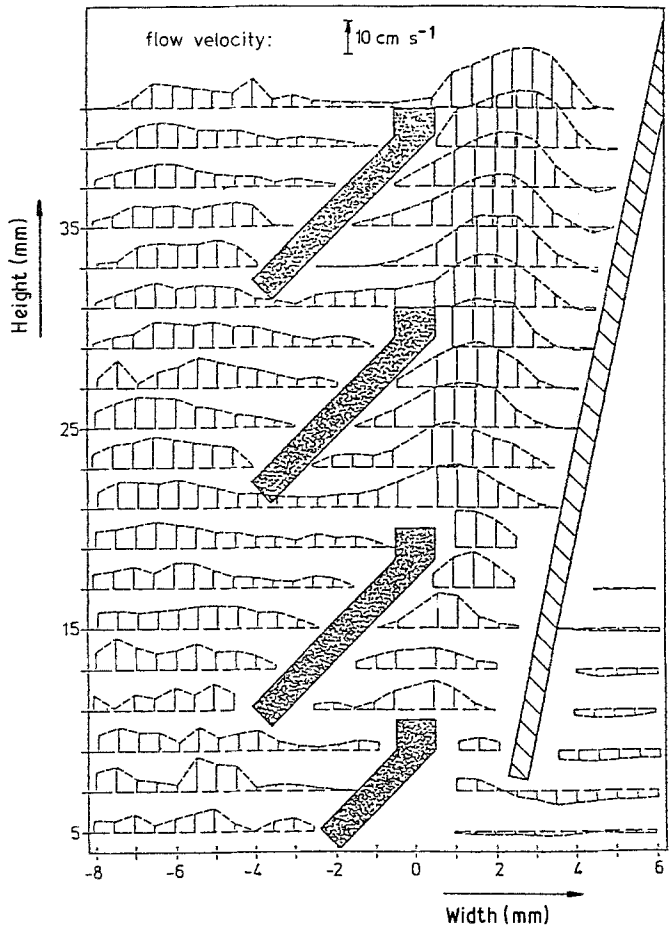

Fig. 8. Vertical velocity distribution at a 'Venetian blind' nickel electrode for hydrogen evolution; 30% KOH.

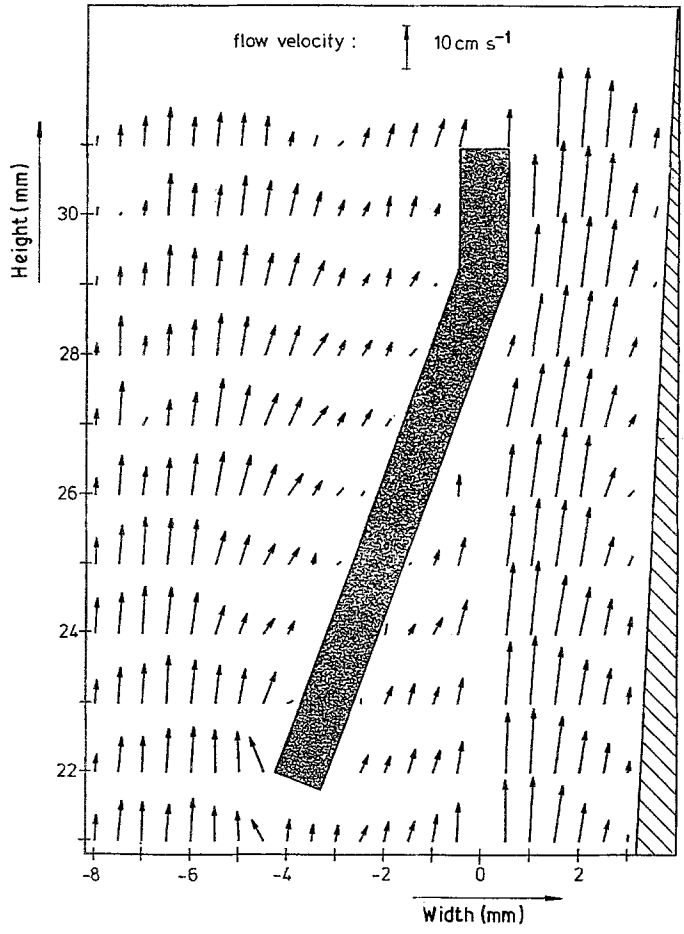

Fig. 9. Velocity distribution at a single slat of the 'Venetian blind' nickel electrode: hydrogen evolution; 30% KOH.

Figure 9 shows the resulting flow vectors on this grid.

Figure 10 clearly shows a flow pattern partially directed towards the electrode backspace induced by the electrode geometry, which reduces the gas load in the electrode separator gap.

An evaluation of data reliability was based on the degree of turbulence, *Tu* [21]. The degree of turbulence can be expressed as the quotient of the standard deviation, s_u, and the mean velocity, $\bar{u}$, for each point in the flow field [22]:

$$Tu = \frac{s_u}{\bar{u}} \text{ with } s_u = \sqrt{\frac{\sum_i (u_i - \bar{u})^2}{N - 1}} \qquad (8)$$

Tu is large in flow regions where the direction is reversed. By statistical data evaluation it was deduced that almost all the measured velocity data have an error of less than 10% with 90% probability [21] which corresponds to a degree of turbulence, *Tu*, of less than 1.92. Only a few data with velocities of about 1 mm s^{-1} and less show a larger degree of turbulence.

4. Conclusions

This investigation demonstrates the important influence of hydrodynamics on electrolysis. The shape of the flow field at a gas-evolving electrode and the velocities therein are strongly affected by geometrical parameters. It has been shown that a disturbance of the flow field by opposite directed flow regions or eddies leads to remarkable velocity decrease of the upward directed flow. The observed velocity gradient perpendicular to a planar electrode surface based on Bernoulli's law results in a force directed towards the electrode surface. This explains the observation of a thin, gas-loaded layer at the electrode surface. The measured velocities are much greater than previously expected [9, 10]. This fast flow field and its dependence on geometrical parameters of the cell and electrodes suggest the possibility of optimization of electrolysis cells by improvement of the gas-diverting effect from the electrode separator gap.

Acknowledgement

The authors would like to acknowledge financial support of this work by Arbeitsgemeinschaft Industrieller Forschungsvereinigungen (AIF) and to thank W. Blatt for helpful assistance in LDA measurements.

References

[1] G. Kreysa and M. Kuhn, *J. Appl. Electrochem.* **15** (1985) 517.
[2] W. Wopersnow and Chr. I. Raub, BMFT Forschungsbericht BMFT-FB W79-31 (1979).
[3] N. Ibl and J. Venczel, *Metalloberfläche* **24** (1970) 365.
[4] H. Vogt, *Electrochim. Acta* **23** (1978) 203.
[5] L. J. J. Janssen and J. G. Hoogland, *Electrochim. Acta* **18** (1973) 543.
[6] I. Rousar and V. Cezner, *Electrochim Acta* **20** (1975) 289.
[7] L. J. J. Janssen, C. W. M. P. Sillen, E. Barendrecht and S. J. D. van Stralen, *Electrochim. Acta* **29** (1984) 633.
[8] H. Vogt, *Electrochim. Acta* **26** (1981) 1311.
[9] B. E. Bongenaar-Schlenter, Thesis, TH Eindhoven (1984).
[10] B. E. Bongenaar-Schlenter, L. J. J. Janssen, S. J. D. van Stralen and E. Barendrecht, *J. Appl. Electrochem.* **15** (1985) 537.
[11] F. Durst and M. Zare, Proc. LDA-Symp., Copenhagen (1975) p. 403.
[12] Y. Yeh and H. Z. Cummins, *Appl. Phys. Lett.* **4** (1964) 176.
[13] R. Buchholz, K. Franz and U. Onken, *Chem. Ing. Tech.* **54** (1982) 154.
[14] K. Franz, Th. Börner, H.-J. Kantorek and R. Buchholz, *Chem. Ing. Tech.* **56** (1984) 154.
[15] Th. Börner, Thesis, Universität Dortmund (1983).
[16] Th. Börner, private communication.
[17] V. G. Levich, 'Physicochemical Hydrodynamics', Prentice-Hall, Englewood Cliffs (1962).
[18] G. Marrucci, *Ind. Eng. Chem. Fundam.* **4** (1965) 224.
[19] Fachlexikon abc Physik, Verlag Harri Deutsch, Thun (1982).
[20] H. Schlichting, Grenzschicht-Theorie, Verlag G. Braun, Karlsruhe (1951).
[21] M. Kuhn, Thesis, Dortmund (1988).
[22] J. Wiedemann, 'Laser-Doppler-Anemometrie', Springer Verlag, Berlin (1984).